LETTER

doi:10.1038/nature11745

Regulation of mTORC1 by the Rag GTPases is necessary for neonatal autophagy and survival

Alejo Efeyan[1,2,3,4,5], Roberto Zoncu[1,2,3,4,5], Steven Chang[1,2,3,4,5], Iwona Gumper[6], Harriet Snitkin[6], Rachel L. Wolfson[1,2,3,4,5], Oktay Kirak[1]†, David D. Sabatini[6] & David M. Sabatini[1,2,3,4,5]

The mechanistic target of rapamycin complex 1 (mTORC1) pathway regulates organismal growth in response to many environmental cues, including nutrients and growth factors[1]. Cell-based studies showed that mTORC1 senses amino acids through the RagA–D family of GTPases[2,3] (also known as RRAGA, B, C and D), but their importance in mammalian physiology is unknown. Here we generate knock-in mice that express a constitutively active form of RagA ($RagA^{GTP}$) from its endogenous promoter. $RagA^{GTP/GTP}$ mice develop normally, but fail to survive postnatal day 1. When delivered by Caesarean section, fasted $RagA^{GTP/GTP}$ neonates die almost twice as rapidly as wild-type littermates. Within an hour of birth, wild-type neonates strongly inhibit mTORC1, which coincides with profound hypoglycaemia and a decrease in plasma amino-acid concentrations. In contrast, mTORC1 inhibition does not occur in $RagA^{GTP/GTP}$ neonates, despite identical reductions in blood nutrient amounts. With prolonged fasting, wild-type neonates recover their plasma glucose concentrations, but $RagA^{GTP/GTP}$ mice remain hypoglycaemic until death, despite using glycogen at a faster rate. The glucose homeostasis defect correlates with the inability of fasted $RagA^{GTP/GTP}$ neonates to trigger autophagy and produce amino acids for *de novo* glucose production. Because profound hypoglycaemia does not inhibit mTORC1 in $RagA^{GTP/GTP}$ neonates, we considered the possibility that the Rag pathway signals glucose as well as amino-acid sufficiency to mTORC1. Indeed, mTORC1 is resistant to glucose deprivation in $RagA^{GTP/GTP}$ fibroblasts, and glucose, like amino acids, controls its recruitment to the lysosomal surface, the site of mTORC1 activation. Thus, the Rag GTPases signal glucose and amino-acid concentrations to mTORC1, and have an unexpectedly key role in neonates in autophagy induction and thus nutrient homeostasis and viability.

The mechanistic target of rapamycin (mTOR) is a serine–threonine kinase that as part of mTORC1 regulates anabolic and catabolic processes required for cell growth and proliferation[1]. mTORC1 integrates signals that reflect the nutritional status of an organism and senses growth factors and nutrients through distinct mechanisms. Growth factors regulate mTORC1 through the PI3K/Akt/TSC1–TSC2 axis, whereas amino acids act through the Rag family of GTPases[2,3]. When activated, these GTPases recruit mTORC1 to the lysosomal surface, an essential step in mTORC1 activation[3,4]. Amino-acid concentrations regulate nucleotide binding to the Rag GTPases in a Ragulator- and vacuolar-type H^+-ATPase-dependent manner[4,5]. In the absence of amino acids, RagA (or RagB, which acts in an identical manner) is loaded with GDP, but becomes bound to GTP when amino acids are plentiful.

To study the physiological importance of the amino-acid-dependent activation of mTORC1, we generated knock-in mice that expressed a constitutively active form of RagA. We chose to manipulate RagA because, although highly similar to RagB, RagA is much more abundant and widely expressed than RagB in mice (Supplementary Fig. 1a). By a single nucleotide substitution in the RagA coding sequence, we replaced glutamine in position 66 with leucine, generating a RagA mutant ($RagA^{Q66L}$) (Supplementary Fig. 1b) that was, regardless of amino-acid concentrations, constitutively active, mimicking a permanent GTP-bound state[3,6] (hereafter referred to as $RagA^{GTP}$). We obtained mouse embryo fibroblasts (MEFs) from embryonic day (E)13.5 embryos and evaluated mTORC1 signalling upon amino-acid or serum deprivation. In $RagA^{+/+}$ and $RagA^{GTP/+}$ cells, deprivation of either amino acids (Fig. 1a) or serum (Supplementary Fig. 1c) suppressed mTORC1 activity, as determined by phosphorylation state of the mTORC1 substrates S6K1 and 4E-BP1. In contrast, in $RagA^{GTP/GTP}$ cells, mTORC1 activity was completely resistant to amino-acid withdrawal (Fig. 1a). However, regulation of PI3K activity by serum was intact, as reflected by Akt phosphorylation (Supplementary Fig. 1c). Interestingly, RagA protein was reduced in $RagA^{GTP/GTP}$ cells, but this was not a consequence of lower $RagA^{GTP}$ messenger (mRNA) expression (Fig. 1b), supporting the existence of a negative feedback triggered by RagA activity. Nevertheless, the cells show the expected amino-acid-independent activation of mTORC1.

Cells lacking the TSC1–TSC2 tumour suppressor complex also have deregulated mTORC1 activity, as such cells maintain mTORC1 signalling in the absence of growth factors[1]. Unlike TSC1- or TSC2-deficient MEFs[7,8], $RagA^{GTP/GTP}$ MEFs have normal proliferation rates without accelerated senescence (Supplementary Fig. 1d). Furthermore, unlike TSC1- or TSC2-deficient embryos, which die at E11.5–E13.5, $RagA^{GTP/GTP}$ embryos were indistinguishable from $RagA^{+/+}$ embryos (Supplementary Fig. 1e), and fetuses were obtained and genotyped at term with the expected Mendelian ratios from heterozygous crosses. Thus, unlike with growth factor sensing, the inability of mTORC1 to sense amino-acid deprivation does not compromise survival during embryonic development, with its steady placental supply of nutrients.

Although apparently not deleterious during *in utero* development, constitutive RagA activity greatly impairs early postnatal survival. Heterozygous $RagA^{GTP/+}$ mice did not have any obvious phenotypic alteration, in agreement with the normal signalling observed in $RagA^{GTP/+}$ MEFs. However, no $RagA^{GTP/GTP}$ mice were obtained at weaning, and were usually found dead within 1 day postpartum in breeding cages. Neonatal death can stem from a variety of defects, so we obtained full-term E19.5 mice by Caesarean section and monitored them outside the breeding cage. Despite having a mild decrease in weight, $RagA^{GTP/GTP}$ neonates were barely distinguishable from control littermates (Fig. 1c, d), and histological analyses showed no abnormalities (Supplementary Fig. 1f).

To understand how constitutive RagA activity affects the regulation of mTORC1 by fasting, we compared the phosphorylation of S6 and 4E-BP1, established markers of mTORC1 activity, in tissues obtained from neonates at birth or fasted for 1 or 10 h. Interestingly, just 1 h of fasting was sufficient to inhibit mTORC1 strongly in $RagA^{+/+}$ and

[1]Whitehead Institute for Biomedical Research, Nine Cambridge Center, Cambridge, Massachusetts 02142, USA. [2]Broad Institute of Harvard and Massachusetts Institute of Technology, Seven Cambridge Center, Cambridge, Massachusetts 02142, USA. [3]Department of Biology, Massachusetts Institute of Technology, Cambridge, Massachusetts 02139, USA. [4]David H. Koch Institute for Integrative Cancer Research at Massachusetts Institute of Technology, 77 Massachusetts Avenue, Cambridge, Massachusetts 02139, USA. [5]Howard Hughes Medical Institute, Massachusetts Institute of Technology, Cambridge, Massachusetts 02139, USA. [6]Department of Cell Biology, New York University School of Medicine, New York, New York 10016-6497, USA. †Present address: The Scripps Research Institute, 10550 North Torrey Pines Road, La Jolla, California 92037, USA.

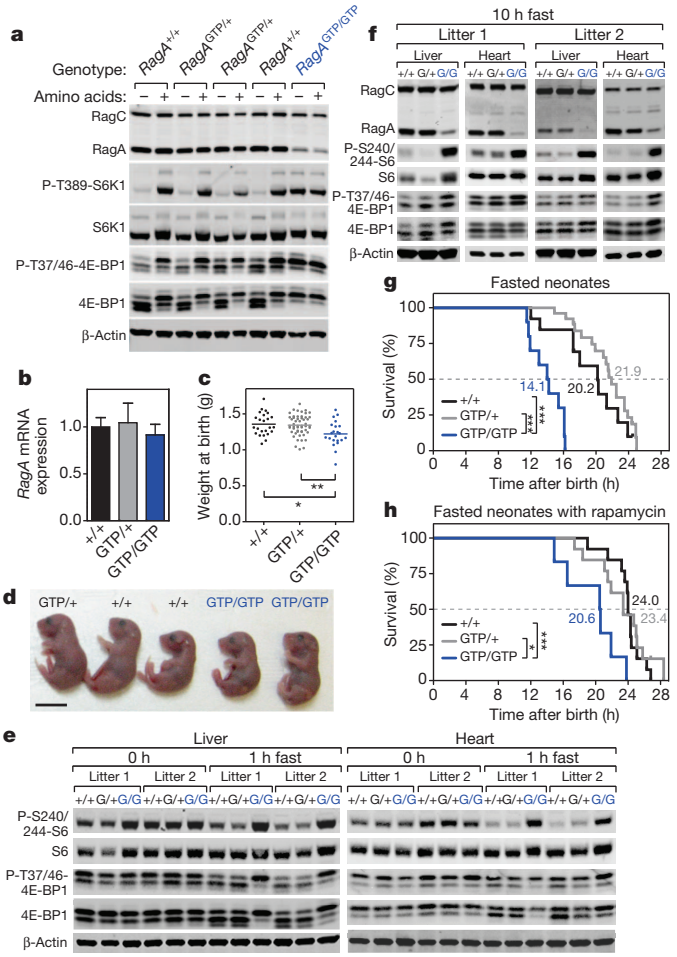

Figure 1 | Characterization of *RagA*$^{GTP/GTP}$ mice. **a**, MEFs of *RagA*$^{+/+}$, *RagA*$^{GTP/+}$ and *RagA*$^{GTP/GTP}$ genotypes were deprived of amino acids for 1 h and re-stimulated for 10 min. Whole-cell protein lysates were immunoblotted for indicated proteins. **b**, Total RNA was extracted from *RagA*$^{+/+}$ ($n = 3$), *RagA*$^{GTP/+}$ ($n = 3$) and *RagA*$^{GTP/GTP}$ ($n = 2$) MEFs and *RagA* mRNA expression determined by quantitative PCR (mean ± s.e.m.). **c**, Weights of *RagA*$^{+/+}$ ($n = 24$), *RagA*$^{GTP/+}$ ($n = 52$) and *RagA*$^{GTP/GTP}$ ($n = 22$) mice at birth (data are scatter dots, mean). **d**, Representative photographs of *RagA*$^{+/+}$, *RagA*$^{GTP/+}$ and *RagA*$^{GTP/GTP}$ neonates. Scale bar, 1 cm. **e**, Early suppression of mTORC1 signalling after birth was determined by immunoblotting of protein extracts from liver and heart of *RagA*$^{+/+}$ (+/+), *RagA*$^{GTP/+}$ (G/+) and *RagA*$^{GTP/GTP}$ (G/G) neonates immediately after Caesarean section (0 h) or after 1 h of fasting (1 h fast). **f**, Liver and heart extracts from *RagA*$^{+/+}$, *RagA*$^{GTP/+}$ and *RagA*$^{GTP/GTP}$ neonates fasted for 10 h were analysed by immunoblotting for the indicated proteins. **g**, Survival curve of fasted neonates. Neonates obtained by Caesarean section and resuscitated were fasted and their survival monitored (+/+: $n = 13$; G/+: $n = 26$; G/G: $n = 10$). **h**, Survival curve of fasted neonates treated with rapamycin. Neonates obtained by Caesarean section and resuscitated were fasted and their survival monitored (+/+: $n = 13$; G/+: $n = 13$; G/G: $n = 6$). Numbers indicate the median survival for each curve. $^*P < 0.05$; $^{**}P < 0.01$; $^{***}P < 0.005$.

RagA$^{GTP/+}$, but not *RagA*$^{GTP/GTP}$, neonates (Fig. 1e and Supplementary Fig. 1g); this difference persisted even after 10 h of fasting (Fig. 1f and Supplementary Fig. 1h). In contrast, Akt phosphorylation was modest at birth and decreased in mice of all genotypes (Supplementary Fig. 1g). As in MEFs, RagA protein was reduced in the tissues of *RagA*$^{GTP/GTP}$ mice, but this again was not due to reduced mRNA levels (Supplementary Fig. 1i). Collectively, these results indicate that constitutive RagA activity causes a profound defect in the response of mTORC1 to fasting.

To examine the consequences of this defect, we fasted neonates for longer periods, which showed that *RagA*$^{GTP/GTP}$ neonates have an accelerated time to death (approximately 14 h for *RagA*$^{GTP/GTP}$ compared with approximately 21 h in *RagA*$^{+/+}$ and *RagA*$^{GTP/+}$) (Fig. 1g). This was not the consequence of unappreciated developmental defects, as the treatment of pups at birth with the mTORC1 inhibitor rapamycin, which suppressed mTORC1 activity in all neonates (Supplementary Fig. 1j), significantly delayed the death of fasted *RagA*$^{GTP/GTP}$ neonates from approximately 14 h to 21 h; $P < 0.01$) (Fig. 1h). These data suggest that Rag-mediated regulation of mTORC1 is necessary for mice to adapt to and survive the starvation period that they endure between birth and feeding.

Consistent with this notion, analysis of blood glucose concentrations showed that fasted *RagA*$^{GTP/GTP}$ neonates suffer a profound defect in nutrient homeostasis. After 1 h of fasting, glycaemia dropped markedly in all neonates to below our 10 mg dl^{-1} limit of detection (Fig. 2a), but by 3–6 h the wild-type animals restored their blood glucose to near birth levels (approximately 40 mg dl^{-1}). In sharp contrast, in *RagA*$^{GTP/GTP}$ neonates, blood glucose concentrations never

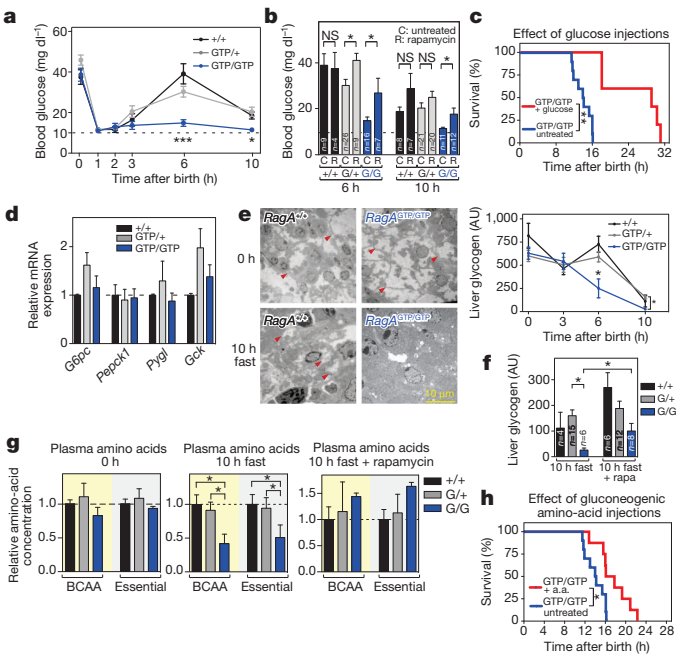

Figure 2 | Profound glucose homeostasis defect in *RagA*$^{GTP/GTP}$ mice. **a**, Glycaemia drop in *RagA*$^{+/+}$, *RagA*$^{GTP/+}$ and *RagA*$^{GTP/GTP}$ and recovery in fasted *RagA*$^{+/+}$ and *RagA*$^{GTP/+}$ but not in *RagA*$^{GTP/GTP}$ neonates (+/+: $n = 5$, 18, 4, 5, 9, 8; G/+: $n = 10$, 26, 10, 13, 26, 21; G/G: $n = 7$, 20, 9, 10, 16, 11, for 0, 1, 2, 3, 6 and 10 h, respectively; mean ± s.e.m.). **b**, Rapamycin significantly increases glycaemia in *RagA*$^{GTP/GTP}$ fasted for 6 and 10 h (mean ± s.e.m.). NS, not significant. **c**, Extension of survival by glucose injections in fasted *RagA*$^{GTP/GTP}$ neonates (untreated: $n = 10$; glucose: $n = 5$). **d**, Normal expression of genes involved in glucose metabolism in neonatal liver (+/+: $n = 2$, G/+: $n = 5$; G/G: $n = 4$; mean ± s.e.m.). **e**, Left: representative electron microscopy images showing abundant glycogen content in *RagA*$^{+/+}$ and *RagA*$^{GTP/GTP}$ hepatocytes before fasting (0 h, upper panels) and more pronounced glycogen depletion after 10 h of fasting (lower panels) in *RagA*$^{GTP/GTP}$ neonates. Right: quantification of hepatic glycogen content (+/+: $n = 5$, 3, 4, 4; G/+: $n = 11$, 7, 14, 15; G/G: $n = 6$, 4, 4, 6; for 0, 3, 6 and 10 h, respectively; mean ± s.e.m.; AU, arbitrary units). **f**, Partial rescue of hepatic glycogen content in *RagA*$^{GTP/GTP}$ neonates fasted for 10 h and treated with rapamycin (rapa) (mean ± s.e.m.). **g**, Quantification of neonatal plasma amounts of branched-chain (BCAA) and essential amino acids at birth (left), after 10 h fasting (middle) and after 10 h fasting with rapamycin treatment (right) (*n* for +/+, G/+ and G/G, respectively: $n = 4$, 5 and 4 for 0 h; $n = 4$, 4 and 3 for 10 h; $n = 2$, 5 and 3 for rapamycin; mean ± s.d.). Values are expressed relative to *RagA*$^{+/+}$ amounts at each time point. **h**, Extension of survival by injection of a combination of gluconeogenic amino acids (a.a.) in fasted *RagA*$^{GTP/GTP}$ neonates (untreated: $n = 10$; amino acids: $n = 8$). $^*P < 0.05$; $^{**}P < 0.01$; ns, $P > 0.05$.

recovered and remained at approximately 10 mg dl^{-1} or lower until death (Fig. 2a). Consistent with its rescue of the accelerated lethality of the *RagA*$^{GTP/GTP}$ neonates during fasting (Fig. 1h), rapamycin administration partly reversed their defect in blood glucose concentrations (Fig. 2b). Moreover, injections of glucose prolonged the lifespan of fasted *RagA*$^{GTP/GTP}$ mice (Fig. 2c), arguing that a lack of glucose has a causal role in their compromised survival.

Because the inability to generate glucose from glycogen can cause perinatal lethality[9], we initially proposed that the *RagA*$^{GTP/GTP}$ neonates had a glycogen metabolism defect. However, *RagA*$^{GTP/GTP}$ neonates did not have defects in the protein or mRNA levels of the key enzymes of glycogen metabolism (Fig. 2d and Supplementary Fig. 2a). Moreover, at birth *RagA*$^{GTP/GTP}$ neonates had normal amounts of hepatic glycogen, which, upon fasting, they consumed at a faster rate than *RagA*$^{+/+}$ and *RagA*$^{GTP/+}$ animals (Fig. 2e), suggesting not a defect in its breakdown but rather accelerated use secondary to hypoglycaemia. As with other characteristics of *RagA*$^{GTP/GTP}$ mice, rapamycin administration partly restored their hepatic glycogen (Fig. 2f).

We also considered defects in gluconeogenesis or the availability of gluconeogenic substrates as potential reasons for the inability of *RagA*$^{GTP/GTP}$ neonates to restore blood glucose concentrations upon fasting. Here too the *RagA*$^{GTP/GTP}$ neonates did not have aberrations in the expression levels of the relevant enzymes (Fig. 2d). However, after a fast for 10 h, *RagA*$^{GTP/GTP}$ neonates did have significantly lower levels of plasma amino acids compared with *RagA*$^{+/+}$ and *RagA*$^{GTP/+}$ littermates (Fig. 2g and Supplementary Fig. 2b). Because murine neonates are born without significant fat stores[10], lipid mobilization cannot serve as a substrate for *de novo* glucose production. Moreover, lactate, another substrate for gluconeogenesis, was not reduced in *RagA*$^{GTP/GTP}$ neonates (Supplementary Fig. 2c), arguing for a specific reduction in amino-acid substrates. As with glucose amounts and glycogen stores (Fig. 2b, f), rapamycin administration reversed the decrease in amino-acid concentrations in *RagA*$^{GTP/GTP}$ neonates (Fig. 2g). Furthermore, injection of a mix of gluconeogenic amino acids, which can contribute to gluconeogenesis but not protein synthesis, delayed the onset of death of *RagA*$^{GTP/GTP}$ neonates (Fig. 2h), and injection of just alanine to fasted neonates provoked a significant increase in glycaemia (Supplementary Fig. 2d). These data are consistent with the glucose homeostasis defect of the fasted *RagA*$^{GTP/GTP}$ neonates being a consequence of reduced circulating amino acids, which leads to lower *de novo* glucose production and plasma levels, and accelerated death.

Several properties of the *RagA*$^{GTP/GTP}$ mice are reminiscent of autophagy-deficient mice[11,12], including the reduction in plasma amino acids and lifespan upon fasting, as well as the slightly lower birth weight. Although mTORC1 negatively regulates autophagy[13], and amino-acid concentrations are regulators of autophagy in rats[14], many mTORC1-dependent and mTORC1-independent autophagy regulators exist[15]. Hence, we wondered if perturbing just one of the several inputs to mTORC1 could exert a dominant effect in the physiological regulation of autophagy.

Quantitative electron microscopy of livers from *RagA*$^{+/+}$ neonates fasted for 1 h showed abundant autophagosomes, characterized by double limiting membranes (Fig. 3a and Supplementary Fig. 3a). Autophagosomes rapidly mature into single-membrane autophagolysosomes, so these were also found in *RagA*$^{+/+}$ livers (Fig. 3a and Supplementary Fig. 3a), albeit the ratio of autophagosomes to autophagolysosomes was high. Both autophagic vacuoles were rarely observed in fasted *RagA*$^{GTP/GTP}$ littermates (Fig. 3a). Similar results were obtained when skeletal muscle was analysed (Fig. 3a).

Even after 10 h of fasting, the autophagy defect in the livers of *RagA*$^{GTP/GTP}$ neonates persisted, as detected by the reduced cleavage of LC3B and degradation of p62 (Fig. 3b), which was increased by administration of rapamycin (Supplementary Fig. 3b). Biochemical analyses for these markers in skeletal and cardiac muscles from *RagA*$^{GTP/GTP}$ neonates after 1 and 2 h of fasting were also consistent with impaired autophagy (Fig. 3c). Cells in culture mirrored the *in vivo*

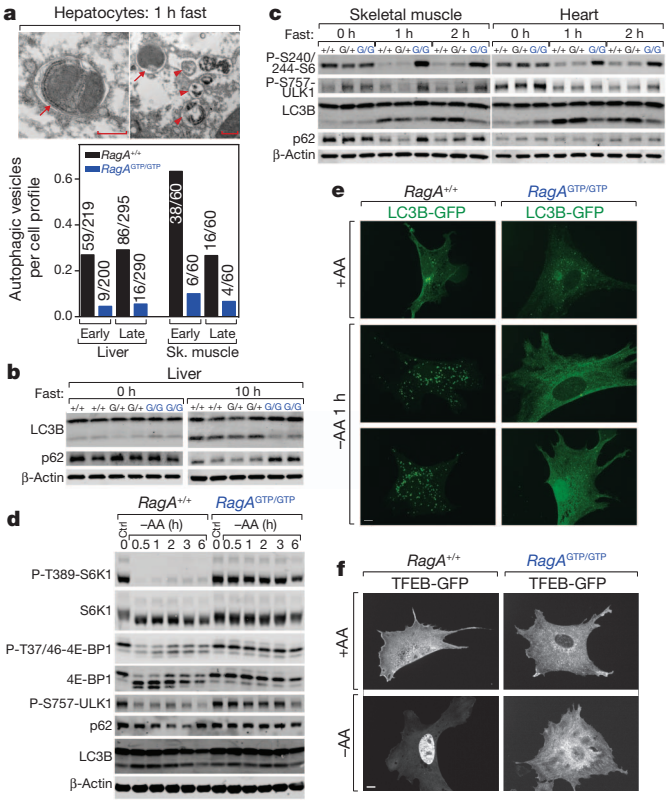

Figure 3 | Impaired autophagy in *RagA*$^{GTP/GTP}$ neonates. **a**, Top: representative micrographs of autophagosomes and autophagolysosomes in hepatocytes from *RagA*$^{+/+}$ neonates fasted for 1 h. Typical autophagosome with a double limiting membrane (arrows); autophagosome and several autolysosomes (arrowheads). Scale bars, 5 μm. Bottom: frequency of the two types of organelle (early: autophagosomes; late: autophagolysosomes) detected in cell profiles of hepatocytes and skeletal myocytes from *RagA*$^{+/+}$ and *RagA*$^{GTP/GTP}$ neonates. **b**, Protein extracts from livers of neonates at Caesarean section (0 h) and fasted for 10 h were immunoblotted for autophagy markers LC3B and p62. **c**, Protein extracts from skeletal muscle and heart from neonates at Caesarean section (0 h), fasted for 1 and 2 h, were immunoblotted for indicated proteins. **d**, Triggering of autophagy by amino-acid withdrawal in MEFs. MEFs were deprived of amino acids for the indicated time points, whole-cell protein extracts were obtained and mTORC1 activity and autophagic activity determined by immunoblotting. **e**, Recombinant LC3B–GFP was expressed in *RagA*$^{+/+}$ and *RagA*$^{GTP/GTP}$ MEFs and LC3B localization, in the presence and absence of amino acids, monitored by fluorescence microscopy. LC3B–GFP (green fluorescent protein) clustering, indicative of autophagy, was observed in amino acid-starved *RagA*$^{+/+}$ but not *RagA*$^{GTP/GTP}$ MEFs. Scale bar, 10 μm. **f**, Localization of recombinant TFEB–GFP was determined in MEFs as in **e**. Nuclear (active) TFEB was observed in *RagA*$^{+/+}$ MEFs upon amino-acid withdrawal.

findings (Fig. 3d), and these results were confirmed by detection of LC3B localization using fluorescence microscopy in amino-acid-starved cells (Fig. 3e and Supplementary Fig. 3c). Consistently, phosphorylation of the autophagy activator ULK-1, a direct substrate of mTORC1 that was suppressed in *RagA*$^{+/+}$ MEFs upon amino-acid withdrawal, remained high in *RagA*$^{GTP/GTP}$ cells (Fig. 3d). In addition, we looked at the transcription factor TFEB, which upregulates genes involved in lysosomal biogenesis and autophagy, but is excluded from the nucleus when phosphorylated by mTORC1 (refs 16, 17). Upon amino-acid deprivation, TFEB localized to the nuclei of *RagA*$^{+/+}$ but not *RagA*$^{GTP/GTP}$ MEFs (Fig. 3f and Supplementary Fig. 3d). This result was mirrored by the decreased expression of TFEB transcriptional targets (Supplementary Fig. 3d).

Serum withdrawal, which inhibits mTORC1 in a Rag-independent fashion, suppressed mTORC1 activity and triggered autophagy in MEFs of all genotypes (Supplementary Fig. 3e), indicating that constitutive

RagA activity does not block autophagy induction by all signals. Thus, despite the multitude of pathways that regulate autophagy[15], Rag GTPase activity upstream of mTORC1 is a major regulator of autophagy *in vivo* during the perinatal period.

Maintenance of mTORC1 activity requires the simultaneous presence of growth factors, amino acids and glucose[1]. We found that after just 1 h of fasting, both plasma amino-acid and glucose concentrations were reduced in neonates of all genotypes (Fig. 2a and Supplementary Fig. 4a). The drop in nutrients correlated with a strong inhibition of mTORC1 activity in $RagA^{+/+}$ and $RagA^{GTP/+}$, but not $RagA^{GTP/GTP}$, neonates (Fig. 1e). Thus, despite a profound hypoglycaemic state, mTORC1 activity remained high in fasted $RagA^{GTP/GTP}$ neonates, a puzzling result given that the Rag GTPases are thought to have a specialized role in amino-acid sensing. These observations led us to consider that the Rag GTPases participate in the direct sensing of glucose concentrations, in addition to their established role in amino-acid sensing. A well-established link between low glucose (but not amino acids (Supplementary Fig. 4b)) and mTORC1 inhibition is the AMP-activated protein kinase (AMPK). However, in MEFs lacking AMPK-α1 and -α2 (AMPK-DKO), mTORC1 activity was still repressed upon glucose deprivation, albeit less prominently than in wild-type MEFs (Fig. 4a). This indicates that an AMPK-independent pathway of mTORC1 inhibition exists, as shown recently in the context of metformin treatment[18]. Compared with control cells, mTORC1 signalling was largely resistant to glucose deprivation in $RagA^{GTP/GTP}$ MEFs (Fig. 4b and Supplementary Fig. 4c, e) and HEK-293T cells expressing $RagB^{GTP}$ (Supplementary Fig. 4d, e). It is unlikely that glucose indirectly inhibits mTORC1 by preventing amino-acid transport, because amino-acid esters, which freely enter cells and substitute for native amino acids in mTORC1 activation[5], did not substitute for glucose (Supplementary Fig. 4f). Moreover, intracellular amino-acid concentrations were only marginally affected in cells deprived of glucose (Supplementary Fig. 4g). In addition, like AMPK-deficient cells[19,20], $RagA^{GTP/GTP}$ cells had enhanced sensitivity to long-term

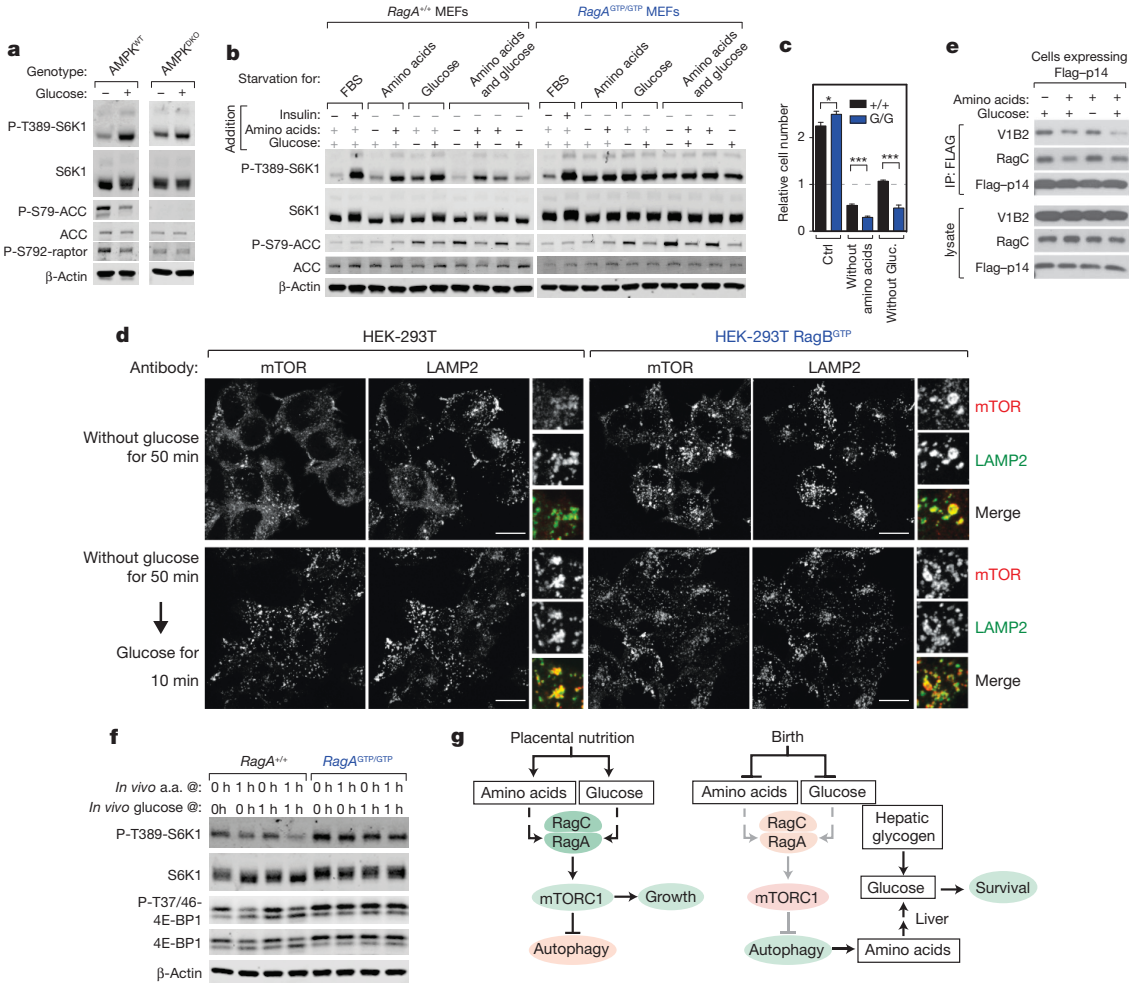

Figure 4 | The Rag GTPases mediate inhibition of mTORC1 by glucose deprivation. **a**, AMPKα1/α2 double knockout (DKO) and wild-type (WT) MEFs were deprived of glucose for 1 h and re-stimulated for 10 min. Whole-cell extracts were immunoblotted for the indicated proteins. **b**, Immortalized MEFs of the indicated genotypes were deprived of growth factors, glucose, amino acids or glucose and amino acids for 1 h and re-stimulated with glucose and/or amino acids for 10 min. Whole-cell lysates were immunoblotted for the indicated proteins. **c**, $RagA^{+/+}$ and $RagA^{GTP/GTP}$ immortalized MEFs were deprived of glucose or amino acids and surviving cells quantified in triplicate after 48 h. Cell number is indicated relative to cell number at the start of the treatment; mean ± s.d.; $***P < 0.005$. **d**, mTOR localization as detected by immunofluorescence. In HEK-293T cells, glucose deprivation causes mTOR to localize to diffuse small puncta throughout the cytoplasm. Re-addition of glucose leads to mTOR shuttling to the lysosomal surface, co-localizing with the lysosomal protein Lamp2. HEK-293T-$RagB^{GTP}$ cells show mTOR localized at the lysosomal surface, regardless of glucose concentrations. Scale bars, 10 μm. **e**, Glucose and amino acids affect the binding of the v-ATPase to the Ragulator complex. HEK-293T expressing Flag-p14 was deprived of glucose or amino acids for 90 min and re-stimulated for 20 min. Protein extracts and immunoprecipitates were immunoblotted for the indicated proteins. **f**, $RagA^{+/+}$ and $RagA^{GTP/GTP}$ primary MEFs were cultured for 1 h in media with the glucose and amino-acid concentrations measured in neonates at birth (0 h) or after fasting for 1 h (1 h) and whole-cell protein extracts were analysed by immunoblotting. **g**, Proposed model for constitutive RagA-induced neonatal lethality. Green and red boxes indicate active and inactive protein or process, respectively.

glucose-deprivation-induced death (Fig. 4c). Constitutive RagA activity does not block AMPK action as aminoimidazole carboxamide ribonucleotide (AICAR), an AMPK activator, inhibited mTORC1 in cells of all genotypes (Supplementary Fig. 4h). In addition, AMPK activity, as monitored by acetyl-CoA carboxylase phosphorylation, was induced to similar amounts in glucose-deprived $RagA^{+/+}$ and $RagA^{GTP/GTP}$ cells (Fig. 4b and Supplementary Fig. 4c), but absent in AMPK-null cells (Fig. 4a). Another cellular nutrient sensor is GCN2 (ref. 21), but although it was regulated by amino acids, it was not by glucose; also, loss of GCN2 did not affect the inhibition of mTORC1 caused by amino-acid or glucose starvation (Supplementary Fig. 4i).

Amino acids promote the Rag-dependent translocation of mTORC1 to the lysosomal surface, a necessary event for its activation[4]. Interestingly, glucose deprivation, like that of amino acids (Supplementary Fig. 4j), rendered mTORC1 diffusely localized in the cytoplasm of HEK-293T cells and, within minutes of glucose re-addition, mTORC1 re-clustered at lysosomes (Fig. 4d). However, in HEK-293T cells expressing $RagB^{GTP}$ and in $RagA^{GTP/GTP}$ MEFs, mTORC1 localized at the lysosomal surface regardless of glucose concentrations (Fig. 4d and Supplementary Fig. 4k). The lysosomal v-ATPase, necessary for the Rag-dependent activation of mTORC1 by amino acids, engages in amino-acid-sensitive interactions with the Ragulator[5], and we found that glucose also regulates the binding of the v-ATPase to Ragulator (Fig. 4e), suggesting a shared regulatory mechanism. Finally, when amino-acid and glucose concentrations at birth and after 1 h neonatal fasting were reproduced in the *in vitro* culture medium, mTORC1 activity was suppressed in $RagA^{+/+}$ but not in $RagA^{GTP/GTP}$ cells placed under the 1 h fasting conditions (Fig. 4f). Hence, we propose that the Rag GTPases are a 'multi-input nutrient sensor', upon which amino acids and glucose converge, in a v-ATPase-dependent manner, upstream of mTORC1.

Altogether, our results support a chain of events that start with the interruption of maternal nutrient supply at birth, which inhibits mTORC1 presumably by converging negative inputs from profound hypoglycaemia and a drop in plasma amino acids, in a Rag-dependent fashion. During the period between birth and suckling, mTORC1 inhibition triggers autophagy, which generates the amino acids used to sustain plasma glucose concentrations through gluconeogenesis. Constitutive RagA activity prevents mTORC1 inhibition, leading to defective autophagy and, thus, insufficient amino-acid production. The lower levels of gluconeogenic amino acids reduce hepatic generation of glucose, which accelerated glycogen breakdown fails to compensate, ultimately leading to hypoglycaemia, energetic exhaustion and accelerated neonatal death (Fig. 4g). Thus, the Rag GTPases have a critical role in nutrient sensing by mTORC1 and in neonatal survival during fasting.

METHODS SUMMARY

All animal studies and procedures were approved by the Massachusetts Institute of Technology Institutional Animal Care and Use Committee. To target the *RagA* locus, we generated a construct consisting of a transcriptional STOP cassette containing the hygromycin resistance gene, flanked by *loxP* sites (*loxP*-*PGK*-*Hyg*-STOP-*loxP*)[22] and placed at 5′ of the *RagA* exon. A RagA activating mutation (Q66L) was generated by an A-to-T substitution in position +197 in the *RagA* exon by site-directed mutagenesis. Chimaeras were crossed to CMV-Cre transgenic mice to allow expression of the $RagA^{Q66L}$ allele. Neonates were obtained by Caesarean section and placed in a humidified chamber at 30 °C and fasted. Subcutaneous injections of rapamycin were performed after Caesarean section, and those of glucose or a mix of gluconeogenic amino acids were performed after Caesarean section and at 3–6 h intervals. Neonatal plasma amino acids were quantified with an Acquity UPLC system (Waters), and hepatic glycogen content as described[23]. For statistical analyses, a log-rank Mantel–Cox method was used for Kaplan–Meier survival curves, and non-parametric *t*-tests and 2×2 χ^2 tests were performed as stated in the legends to the figures.

Full Methods and any associated references are available in the online version of the paper.

Received 15 February; accepted 5 November 2012.
Published online 23 December 2012.

1. Zoncu, R., Efeyan, A. & Sabatini, D. M. mTOR: from growth signal integration to cancer, diabetes and ageing. *Nature Rev. Mol. Cell Biol.* **12,** 21–35 (2010).
2. Kim, E., Goraksha-Hicks, P., Li, L., Neufeld, T. P. & Guan, K. L. Regulation of TORC1 by Rag GTPases in nutrient response. *Nature Cell Biol.* **10,** 935–945 (2008).
3. Sancak, Y. *et al.* The Rag GTPases bind raptor and mediate amino acid signaling to mTORC1. *Science* **320,** 1496–1501 (2008).
4. Sancak, Y. *et al.* Ragulator-Rag complex targets mTORC1 to the lysosomal surface and is necessary for its activation by amino acids. *Cell* **141,** 290–303 (2010).
5. Zoncu, R. *et al.* mTORC1 senses lysosomal amino acids through an inside-out mechanism that requires the vacuolar H-ATPase. *Science* **334,** 678–683 (2011).
6. Hirose, E., Nakashima, N., Sekiguchi, T. & Nishimoto, T. RagA is a functional homologue of *S. cerevisiae* Gtr1p involved in the Ran/Gsp1-GTPase pathway. *J. Cell Sci.* **111,** 11–21 (1998).
7. Kwiatkowski, D. J. *et al.* A mouse model of TSC1 reveals sex-dependent lethality from liver hemangiomas, and up-regulation of p70S6 kinase activity in Tsc1 null cells. *Hum. Mol. Genet.* **11,** 525–534 (2002).
8. Zhang, H. *et al.* Loss of Tsc1/Tsc2 activates mTOR and disrupts PI3K-Akt signaling through downregulation of PDGFR. *J. Clin. Invest.* **112,** 1223–1233 (2003).
9. Scheuner, D. *et al.* Translational control is required for the unfolded protein response and in vivo glucose homeostasis. *Mol. Cell* **7,** 1165–1176 (2001).
10. Birsoy, K. *et al.* Analysis of gene networks in white adipose tissue development reveals a role for ETS2 in adipogenesis. *Development* **138,** 4709–4719 (2011).
11. Kuma, A. *et al.* The role of autophagy during the early neonatal starvation period. *Nature* **432,** 1032–1036 (2004).
12. Komatsu, M. *et al.* Impairment of starvation-induced and constitutive autophagy in *Atg7*-deficient mice. *J. Cell Biol.* **169,** 425–434 (2005).
13. Mizushima, N., Levine, B., Cuervo, A. M. & Klionsky, D. J. Autophagy fights disease through cellular self-digestion. *Nature* **451,** 1069–1075 (2008).
14. Mortimore, G. E. & Schworer, C. M. Induction of autophagy by amino-acid deprivation in perfused rat liver. *Nature* **270,** 174–176 (1977).
15. Kroemer, G., Marino, G. & Levine, B. Autophagy and the integrated stress response. *Mol. Cell* **40,** 280–293 (2010).
16. Roczniak-Ferguson, A. *et al.* The transcription factor TFEB links mTORC1 signaling to transcriptional control of lysosome homeostasis. *Sci. Signal.* **5,** ra42 (2012).
17. Settembre, C. *et al.* A lysosome-to-nucleus signalling mechanism senses and regulates the lysosome via mTOR and TFEB. *EMBO J.* **31,** 1095–1108 (2012).
18. Kalender, A. *et al.* Metformin, independent of AMPK, inhibits mTORC1 in a rag GTPase-dependent manner. *Cell Metab.* **11,** 390–401 (2010).
19. Choo, A. Y. *et al.* Glucose addiction of TSC null cells is caused by failed mTORC1-dependent balancing of metabolic demand with supply. *Mol. Cell* **38,** 487–499 (2010).
20. Shaw, R. J. *et al.* The tumor suppressor LKB1 kinase directly activates AMP-activated kinase and regulates apoptosis in response to energy stress. *Proc. Natl Acad. Sci. USA* **101,** 3329–3335 (2004).
21. Proud, C. G. eIF2 and the control of cell physiology. *Semin. Cell Dev. Biol.* **16,** 3–12 (2005).
22. Guerra, C. *et al.* Tumor induction by an endogenous *K-ras* oncogene is highly dependent on cellular context. *Cancer Cell* **4,** 111–120 (2003).
23. Lo, S., Russell, J. C. & Taylor, A. W. Determination of glycogen in small tissue samples. *J. Appl. Physiol.* **28,** 234–236 (1970).

Supplementary Information is available in the online version of the paper.

Acknowledgements We thank members of the Sabatini laboratory for suggestions, and A. Hutchins for technical assistance. We thank R. Shaw for providing the AMPK-DKO MEFs, D. Ron for the GCN2-KO MEFs and M. Barbacid for the transcriptional STOP cassette. This work was supported by grants from the National Institutes of Health (R01 CA129105, R01 CA103866 and R37 AI047389) and awards from the American Federation for Aging, Starr Foundation, Koch Institute Frontier Research Program, and the Ellison Medical Foundation to D.M.S., fellowships from the Human Frontiers Science Program to A.E., and the Jane Coffin Childs Memorial Fund for Medical Research and the LAM Foundation to R.Z. D.M.S. in an investigator of Howard Hughes Medical Institute.

Author Contributions A.E. and D.M.S. conceived the project. A.E. designed and performed most experiments with input from D.M.S, and assistance from S.C., R.L.W. and O.K. R.Z. performed experiments and participated in discussion of the results. I.G., H.S. and D.D.S. performed electron microscopy experiments and interpretations. D.D.S. helped with discussion and interpretation of results. A.E. wrote and D.M.S. edited the manuscript.

Author Information Reprints and permissions information is available at www.nature.com/reprints. The authors declare no competing financial interests. Readers are welcome to comment on the online version of the paper. Correspondence and requests for materials should be addressed to D.M.S. (sabatini@wi.mit.edu).

METHODS

Generation of *RagA*^{GTP} mice. All animal work was performed in accordance with the Massachusetts Institute of Technology Committee on Animal Care. To target the *RagA* locus, we generated a construct consisting of a 4-kilobase 5′ homology arm upstream of the *RagA* gene, a transcriptional STOP cassette containing a the hygromycin resistance gene, flanked by *loxP* sites (*loxP-PGK-Hyg*-STOP-*loxP*)[22] placed at the 5′ end of the *RagA* exon, followed by a 3-kilobase 3′ homology arm downstream of *RagA* genomic sequence. For cloning purposes, a NotI restriction (GCGGCCGC) site was inserted into the 5′ homology arm, replacing the GGCGACGC sequence located 17 nucleotides upstream of the *RagA* ATG translation start codon. The *loxP-PGK-Hyg*-STOP-*loxP*, previously cloned in the pMeca plasmid, was excised with NotI and inserted in the *RagA* construct. An A-to-T substitution in position +197 in *RagA* exon was performed by site-directed mutagenesis. This mutation translates into a Q66L amino-acid substitution that renders a RagA protein that is constitutively active. See also Supplementary Fig. 1b. The construct was inserted into pPGKNeo.F2L2.DTA, linearized with XmaI and electroporated into male embryonic stem cells of mixed 129Sv/C57B6 background. Embryonic stem cell colonies were picked and identified by Southern blot and confirmed by PCR amplification of specific insertion products. Positive embryonic stem cell clones were then injected into blastocysts and transferred into pseudo-pregnant females to obtain chimaeric mice. Male chimaeras were crossed to CMV-Cre transgenic females of C57BL/6J background, resulting in excision of the transcriptional STOP cassette and allowing expression of the *RagA*^{Q66L} allele, then intercrossed.

Preparation of MEFs. MEFs from E13.5 embryos of *RagA*$^{+/+}$, *RagA*$^{GTP/+}$ and *RagA*$^{GTP/GTP}$ genotype were prepared by chemical digestion followed by mechanical disaggregation. For spontaneous immortalization, MEFs were re-plated every 3 days until senescent. Spontaneously proliferating cells eventually arose after a senescent phase. AMPKα1/α2 DKO immortalized MEFs and matched wild-type MEFs were provided by R. Shaw; D. Ron provided the GCN2 KO MEFs.

Amino-acid, glucose and serum starvation and stimulation of cells. For amino acids and/or glucose deprivation in MEFs, sub-confluent cells were rinsed twice and incubated in RPMI without amino acids, glucose or both, and supplemented with 10% dialysed FBS, as described[3]. Stimulation with glucose (5 mM) or amino acids (concentration as in RPMI) was performed for 10 min, unless otherwise indicated. For serum withdrawal, cells were rinsed twice in serum-free DMEM and incubated in serum-free DMEM for the indicated times; 100 nM was used for insulin stimulation. Aminoimidazole carboxamide ribonucleotide (AICAR, EMD Biosiences) was used at a final concentration of 2 mM. For cell survival experiments, cells were deprived of glucose or amino acids, and attached cells were counted 48 h later. For treatments with *in vivo* concentration of nutrients, MEFs were incubated with the following concentrations of amino acids (all in μM), reflecting the values found at birth (0 h) and after fasting for 1 h (1 h) in control mice: 0 h: D, 34; T, 446; S, 268; N, 180; E, 194; Q, 1221; P, 289; G, 382; V, 321; C, 26; M, 245; I, 122; L, 192; Y, 165; F, 189; W, 124; K, 1026; H, 74; R, 199; 1 h: D, 48; T, 172; S, 82; N, 57; E, 128; Q, 592; P, 183; G, 298; V, 154; C, 17; M, 164; I, 26; L, 37; Y, 71; F, 72; W, 92; K, 723; H, 30; R, 78. Similarly, the concentrations of glucose were as follows: 0 h: 45 mg dl^{-1}; 1 h: 12 mg dl^{-1}. Protein extracts were obtained as above.

Immunoblotting. Reagents were obtained from the following sources: anti phospho-T389 S6K1, phospho-S240/244 S6, phospho-T37/T46 4E-BP1, phospho-T308 Akt, phospho-S473 Akt, phospho-S757 ULK1, phospho-S9 GSK3-β, phospho-S641 glycogen synthase, phospho-S51-eIF2a, total Akt, S6K1, 4E-BP1, GSK3-β, glycogen synthase and eIF2a from Cell Signaling Technology; anti LC3B from Cell Signaling Technology and Novus Biologicals; anti β-actin (clone AC-15) from Sigma; anti p62 from America Research Products, Cell Signaling Technology and Enzo Life Sciences; anti PYGL from Santa Cruz. Cells were rinsed once with ice-cold PBS and lysed in ice-cold lysis buffer (50 mM HEPES (pH 7.4), 40 mM NaCl, 2 mM EDTA, 1.5 mM sodium orthovanadate, 50 mM NaF, 10 mM pyrophosphate, 10 mM glycerophosphate and 1% Triton X-100, and one tablet of EDTA-free complete protease inhibitors (Roche) per 25 ml). Cell lysates were cleared by centrifugation at 15,000*g* for 10 min. Protein extracts were denatured by the addition of sample buffer, boiled for 5 min, resolved by SDS–polyacrylamide gel electrophoresis and analysed by immunoblotting.

Immunofluorescence assays in cells. MEFs or HEK-293T cells were plated on fibronectin-coated 2 cm^2 glass coverslips at a density of 50,000–100,000 cells per coverslip. For overexpression of GFP–LC3B and TFEB–GFP, cells were transfected with nucleofection (Lonza) using 1 μg for 2×10^6 cells. The following day, cells were transferred to amino-acid- or glucose-free RPMI, starved for 60 min or starved for 50 min and re-stimulated for 10 min with amino acids or glucose, rinsed with cold PBS once and fixed for 15 min with 4% paraformaldehyde. Coverslips were permeabilized with 0.05% Triton X-100 in PBS and then incubated with primary antibodies in 5% normal donkey serum for 1 h, rinsed and incubated with Alexa Fluor-conjugated secondary antibodies (Invitrogen) diluted 1:400, for 45 min. Cells overexpressing GFP–LC3B and TFEB–GFP were fixed in 4% paraformaldehyde, rinsed and imaged. Coverslips were mounted on glass slides using Vectashield (Vector Laboratories) and imaged on a spinning disk confocal system (Perkin Elmer) equipped with 405, 488 and 561 nm laser lines, through a ×63 objective.

Co-immunoprecipitation assays. HEK-293T cells stably expressing Flag-tagged proteins were processed as described[5].

Quantitative PCR. Total RNA was extracted with RNeasy (Qiagen), retrotranscribed with Superscript III (Invitrogen) and used at 1:100 dilution in quantitative real-time PCR in an Applied Biosystems thermocycler. 36B4 and β-actin were for normalization. The following primers were used: *RagA* F, GAACC TGGTGCTGAACCTGT; *RagA* R, GATGGCTTCCAGACACGATT; *RagB* F, TTCGATTTCTGGGAAACCTG; *RagB* R, AGTTCACGGCTCTCCACATC; mTOR F, GGTGCTGACCGAAATGAGGG; mTOR (also known as *Mtor*) R, TCTTGCCCTTGTGTTCTGCA; *Raptor* (also known as *Rptor*) F, TGGC AGCCAAGGGCTCGGTA; *Raptor* R, GCAGCAGCTCGTGTGCCTCA; *Rictor* F, TCGCAACTCACCACAAGCGGG; *Rictor* R, TGCAAGCATCTGTGG CTGCCG; *Pepck1* F, CGATGACATCGCCTGGATGA; *Pepck1* R, TCTTGC CCTTGTGTTCTGCA; *G6pc* F, GAAGGCCAAGAGATGGTGTGA; *G6pc* R, TGCAGCTCTTGCGGTACATG; glucokinase F, GAGATGGATGTGGTGGC AAT; glucokinase R, ACCAGCTCCACATTCTGCAT; *36B4* (also known as *Rplp0*) F, TAAAGACTGGAGACAAGGTG; *36B4* R, GTGTACTCAGTCT CCACAGA; *Sqstm1* F, GAACTCGCTATAAGTGCAGTGT; *Sqstm1* R, AGAGA AGCTATCAGAGAGGTGG; *Vps11* F, GGAGCCTGGTCTTTGGAGA; *Vps11* R, GCTGTAGAGAACGTGGCAAGA; *Vps33a* F, TCTGTGCTCAGCAAGAA GGCGA; *Vps33a* R, GGACGCAAACTGCTTGATCTCC; *Vps8* F, GATGGACC ATCTCCTGAAACAGG; *Vps8* R, AGCCTTCCTCTTGCTGACATCC; *Uvrag* F, GGAATAATGCCGGATCGTCTG; *Uvrag* R, CCTTTCCACCCCAAATCTT CAC; actin F, GGCACCACACCTTCTACAATG; actin R, GTGGTGGT GAAGCTGTAGCC.

Neonatal fasting and treatments. E17.5 and E18.5 pregnant females were injected with 2 mg progesterone (Sigma-Aldrich) to prevent early delivery. At E19.5, females were euthanized and fetuses immediately obtained by Caesarean section. Successfully resuscitated neonates were placed in a humidified chamber at 30 °C and fasted. Rapamycin (LC Laboratories) was administered intraperitoneally at a volume of 100 μl (1 mg ml^{-1} concentration) to pregnant females 4 h before Caesarean section, and neonates were injected subcutaneously immediately after Caesarean section. Glucose (30%) in PBS, or gluconeogenic amino acid mix (A, 500 mg ml^{-1}; N, 10 mg ml^{-1}; S, 6 mg ml^{-1}; D, E and P, 4 mg ml^{-1}; G, 2 mg ml^{-1}) in PBS, were injected subcutaneously every 3–6 h.

Electron microscopy. Tissues were obtained and immediately fixed in 2% glutaraldehyde in 0.1 M sodium cacodylate buffer pH 7.4 at room temperature. After post-fixation in 2% OsO_4, blocks were processed for embedding in Epon 812. Thin sections were obtained, stained with uranyl acetate and lead citrate, and examined by transmission electron microscopy in a JEOL EX 1200 electron microscope.

Measurement of glucose and amino-acid concentrations. Blood glucose was quantified with a glucometer and glucose test strips (Bayer Contour), with a lower detection limit of 10 mg dl^{-1}. For amino-acid quantification, plasma was analysed using the Waters MassTrak Amino Acid system. Pre-column derivatization of amino acids through molar excess of 6-aminoquinolyl-*N*-hydroxysuccinimidyl carbamate was performed, converting both primary and secondary amino acids to stable chromophores. The derivatized amino acids were separated and detected using an Acquity UPLC system (Waters) and ultraviolet absorbance. Amino-acid concentrations in MEFs were quantified in the same manner after total extraction in boiling distilled H_2O.

Hepatic glycogen content measurement. Glycogen was measured in liver samples as described[23]. Briefly, glycogen was extracted from neonatal livers in 30% KOH saturated with Na_2SO_4, precipitated in 95% ethanol and re-suspended in double-distilled H_2O. After addition of phenol and H_2SO_4, absorbance at 490 nm was measured in triplicates.

Statistical analyses. For Kaplan–Meier survival curves, comparisons were made with the log-rank Mantel–Cox method. For quantitative PCR, measurements of glycaemia, plasma amino acids and glycogen content, non-parametric *t*-tests were performed. χ^2 tests were also performed for the effects of rapamycin on glycaemia.

SUPPLEMENTARY INFORMATION

doi:10.1038/nature11745

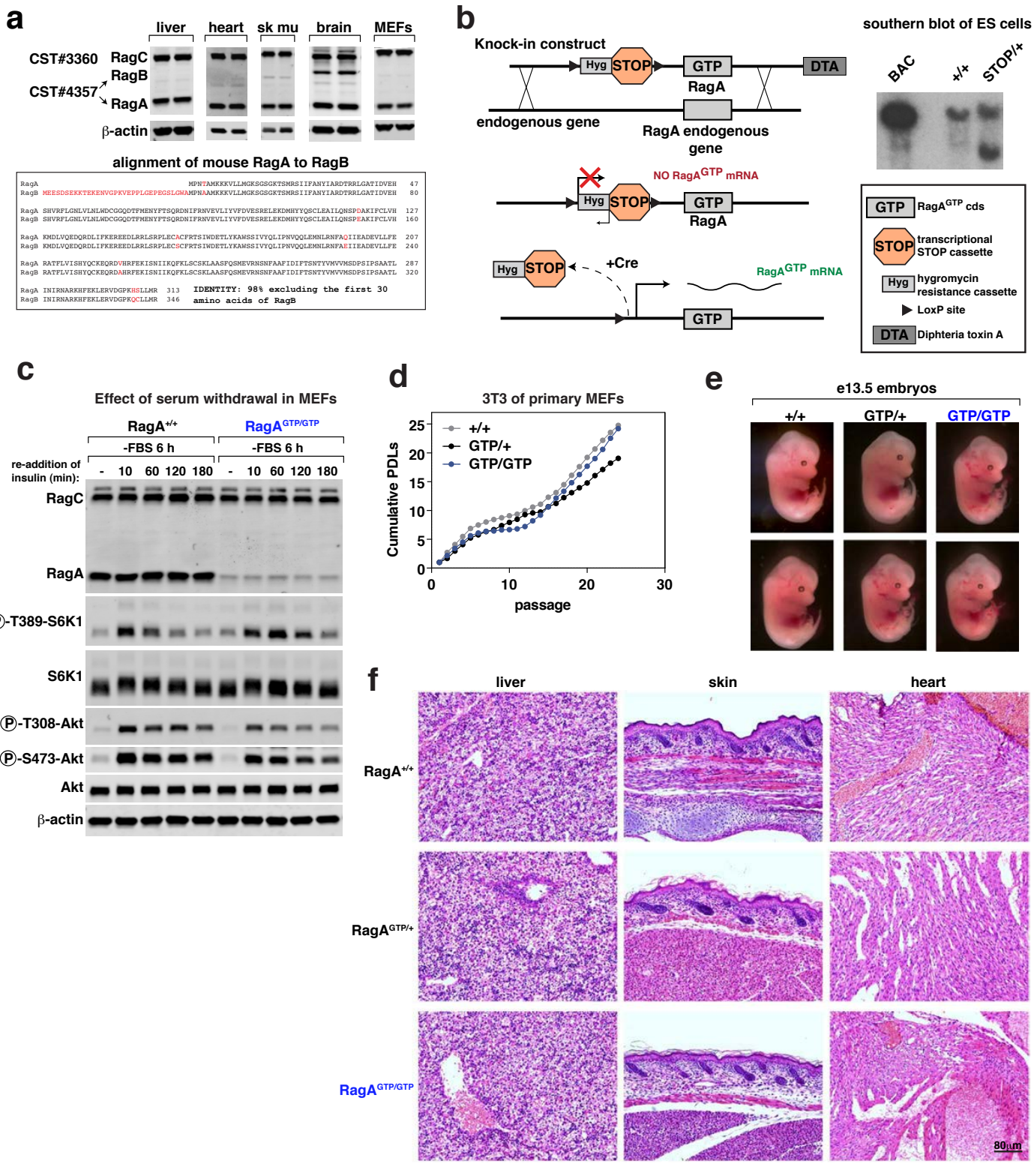

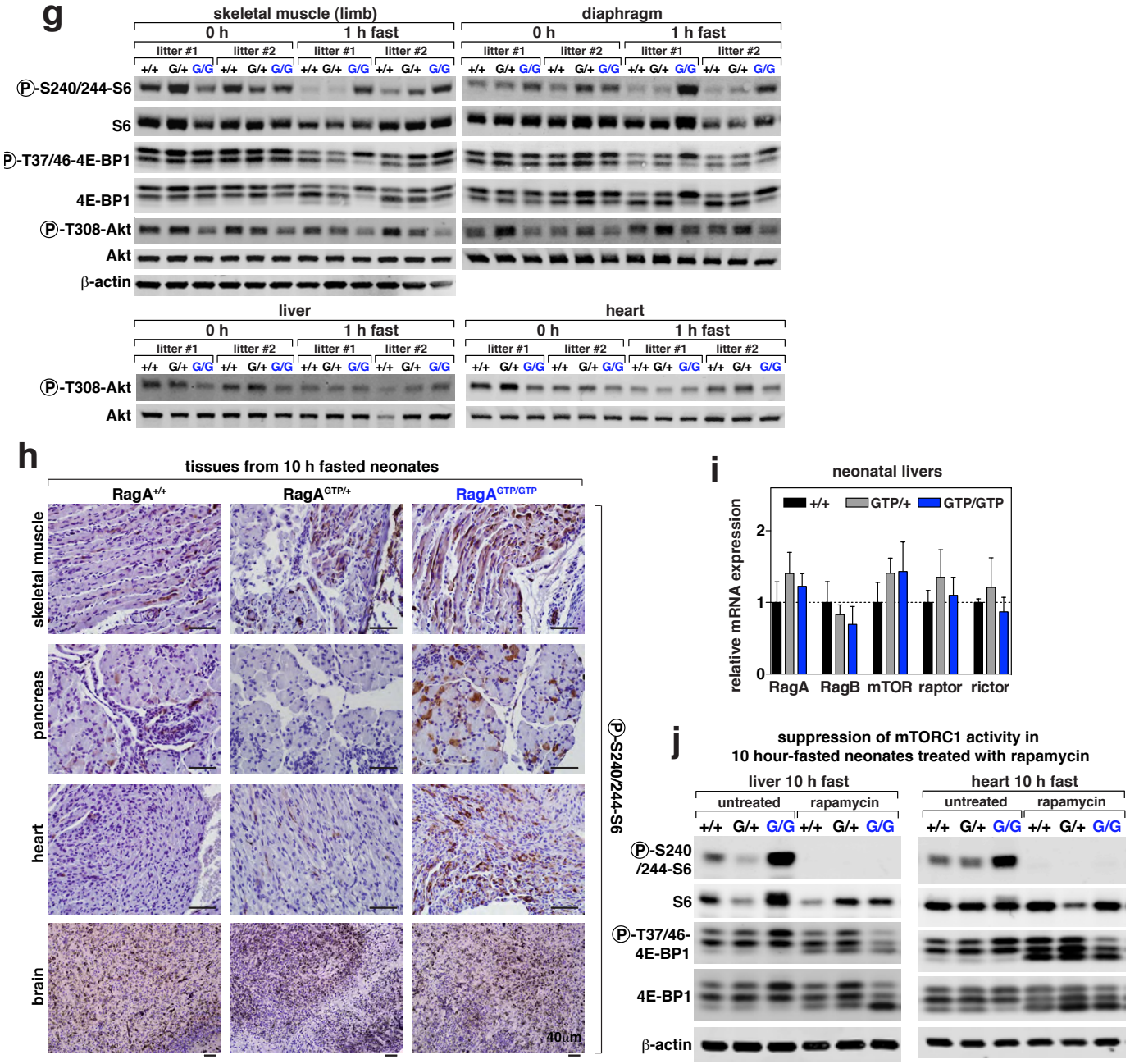

Supplementary Figure 1. (A) (Top) Protein levels of RagA, RagB and RagC in tissues and MEFs. Note that significant RagB levels are found only in brain. (Bottom) Alignment of mouse RagA to RagB proteins. Except for the n-terminus extension in RagB, identity is ~98%. **(B)** Strategy for RagA knock-in construct and recombination. Southern blot of ES cells was performed using EcoRV as restriction enzyme, which cuts in the transcriptional STOP cassette, and a 5' probe. **(C)** MEFs of all genotypes show inhibition of mTORC1 activity upon serum withdrawal. Cells were deprived of FBS for 6 h and FBS was re-added for indicated times points and whole-cell protein extracts were obtained. **(D)** 3T3 protocol performed in RagA$^{+/+}$, RagA $^{GTP/+}$ and RagA$^{GTP/GTP}$ MEFs. **(E)** Representative pictures of RagA$^{+/+}$, RagA$^{GTP/+}$ and RagA$^{GTP/GTP}$ E13.5 embryos. **(F)** Hematoxylin & eosin staining of liver, skin, heart and brain of RagA$^{+/+}$, RagA$^{GTP/+}$ and RagA$^{GTP/GTP}$ neonates. **(G)** (Top) Lack of inhibition of mTORC1 activity by 1 h fasting in RagA$^{GTP/GTP}$ neonatal skeletal muscle from leg and diaphragm. (Bottom) Akt signaling in 1 h fasted neonatal liver and heart. **(H)** High mTORC1 activity (p-S6) in tissues from RagA$^{GTP/GTP}$ neonates (versus RagA$^{+/+}$ and RagA$^{GTP/+}$ neonates) after 10 h fasting. **(I)** mRNA expression by qtRT-PCR in livers from RagA$^{+/+}$ (n=2), RagA$^{GTP/+}$ (n=5) and RagA$^{GTP/GTP}$ (n=4) neonates; data are mean ± SEM. **(J)** Suppression of mTORC1 activity by rapamycin in liver and heart from RagA$^{+/+}$, RagA$^{GTP/+}$ and RagA$^{GTP/GTP}$ neonates.

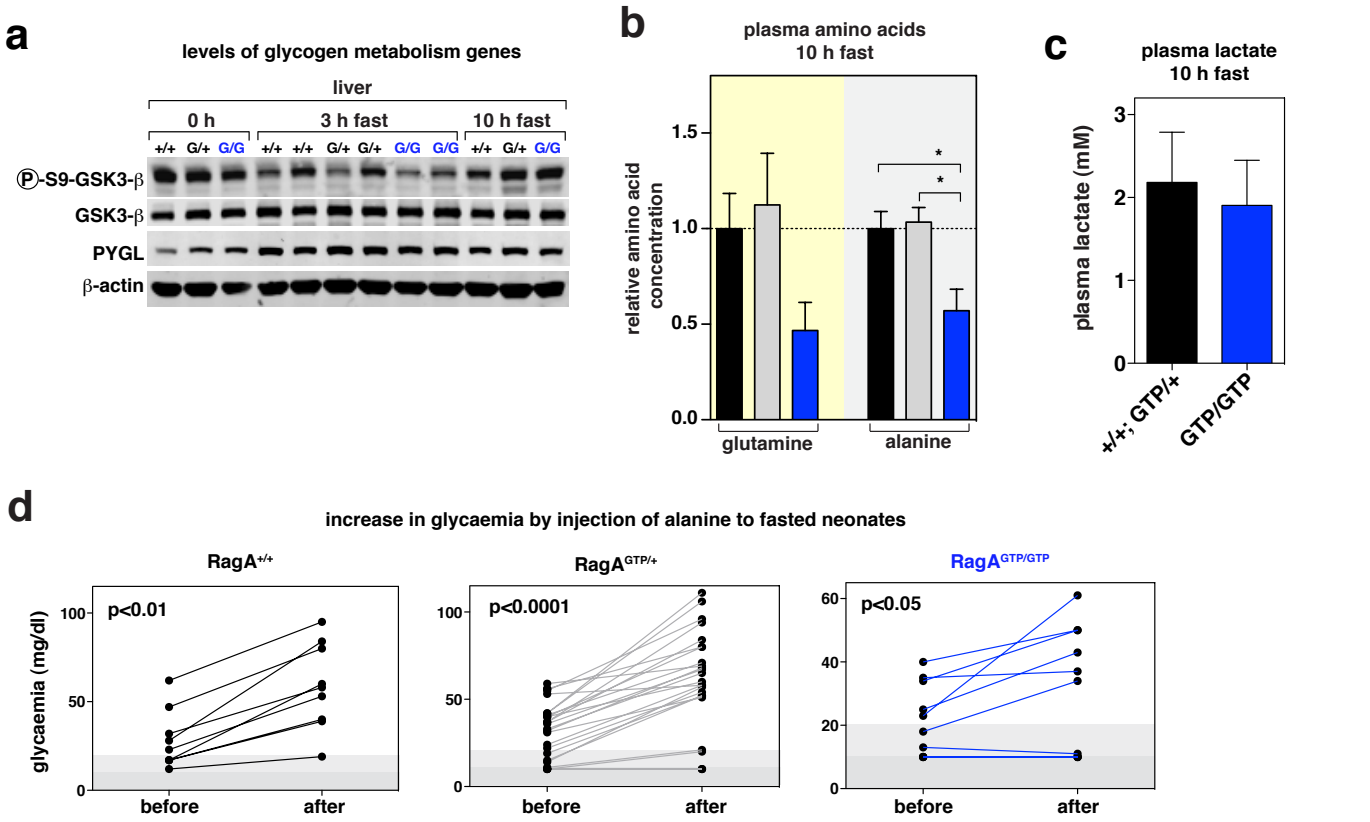

Supplementary Figure 2. (A) Western blot of genes involved in glycogen metabolism. **(B)** Reduced levels of plasma glutamine and alanine in and RagA$^{GTP/GTP}$ neonates fasted for 10 h (n=4, n=4 and n=3, respectively; data are mean ± SEM). **(C)** Similar levels of plasma lactate in RagA$^{GTP/GTP}$ (n=3) versus RagA$^{+/+}$ and RagA$^{GTP/+}$ (n=4) neonates fasted 10 h, data are mean ± SD. **(D)** Proficient gluconeogenesis in neonates by amino acid substrates. Fifteen-percent alanine in PBS was injected after 5.5 h of fasting and 45 min later; glycaemia was measured immediately before the first injection and 75 min later. All neonates, regardless of the genotype, undergo a significant increase in glycaemia, reflecting the ability to execute gluconeogenesis from amino acid substrates (+/+: n=9, G/+: n=26; G/G: n=11; some values overlap).

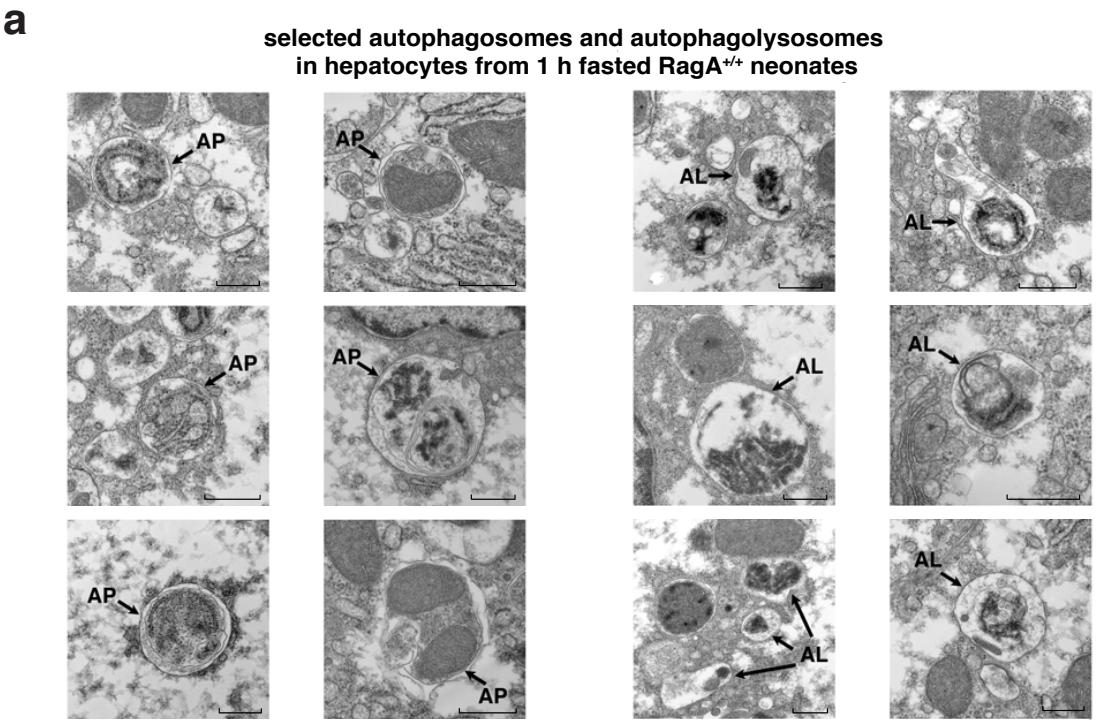
a
selected autophagosomes and autophagolysosomes
in hepatocytes from 1 h fasted RagA+/+ neonates
AP
AL

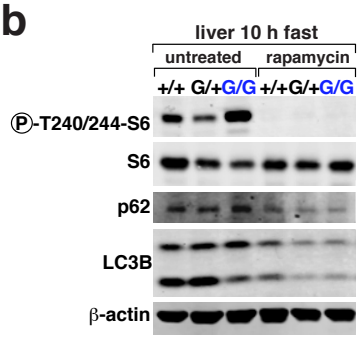
b
liver 10 h fast
untreated
rapamycin
+/+ G/+G/G +/+G/+G/G
Ⓟ-T240/244-S6
S6
p62
LC3B
β-actin

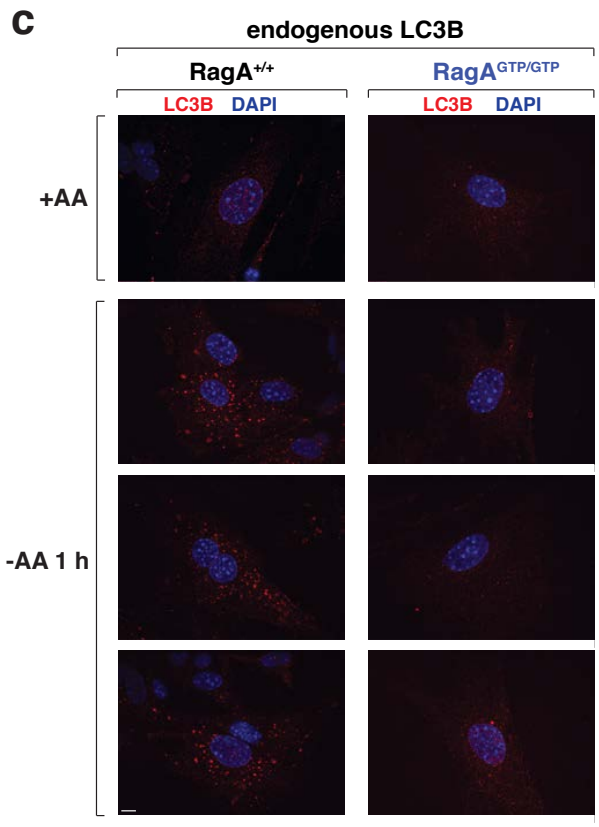
c
endogenous LC3B
RagA+/+
RagAGTP/GTP
LC3B DAPI
+AA
-AA 1 h

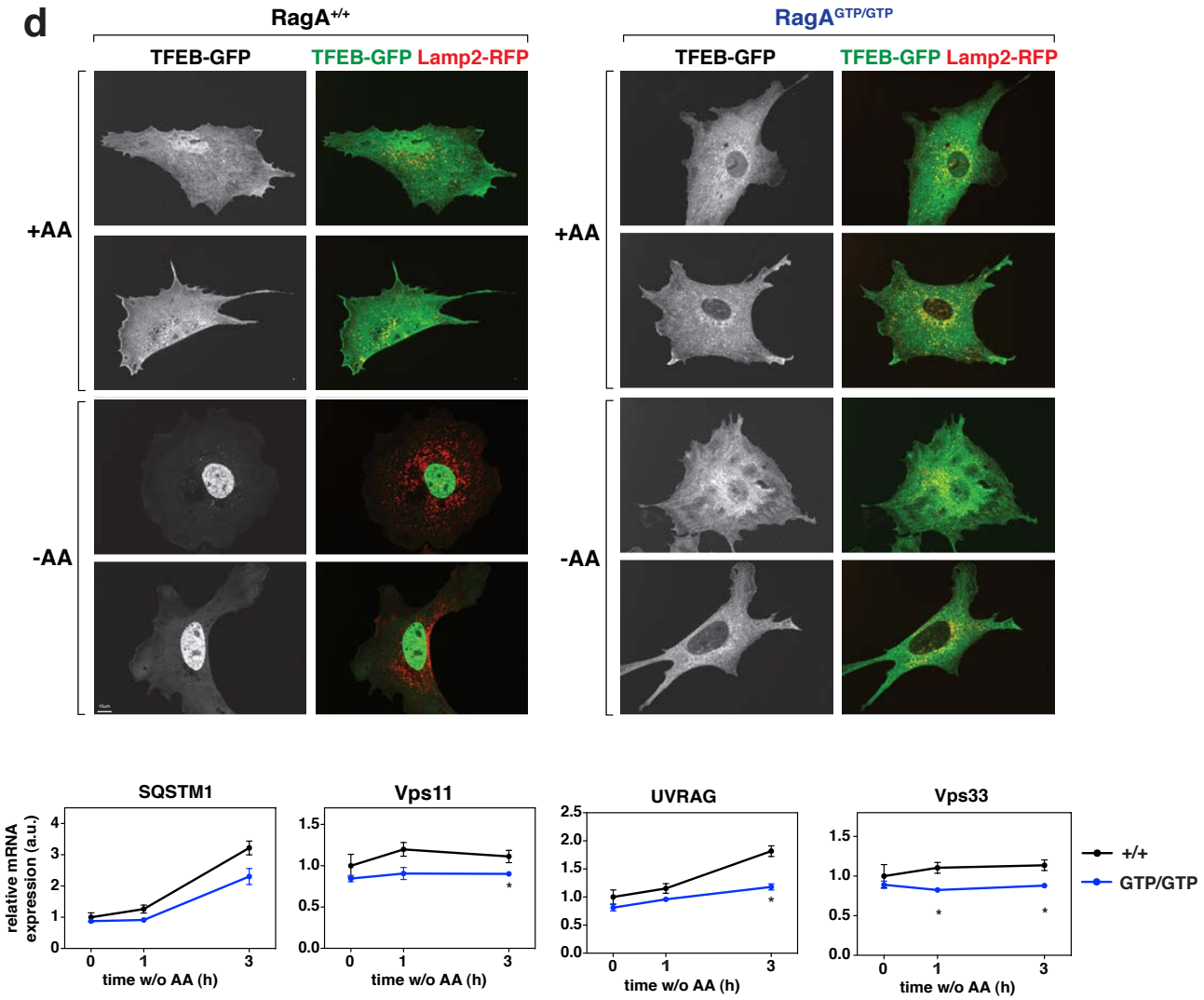

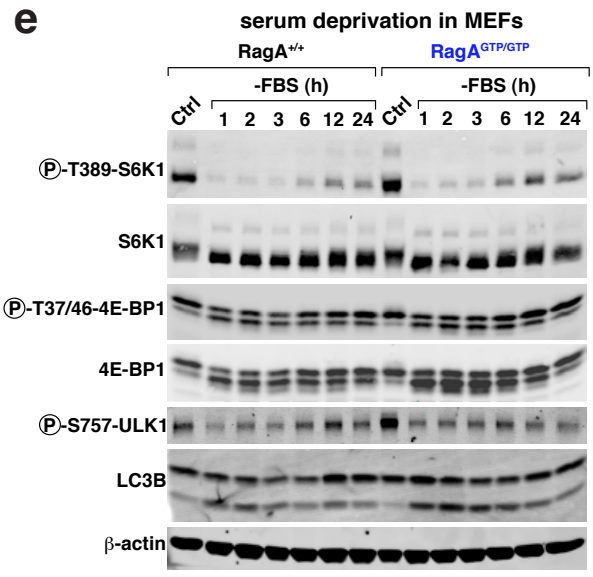

Supplementary Figure 3. (A) Representative electron micrographs of RagA$^{+/+}$ livers showing autophagosomes (AP) and autophagolysosomes (AL). Bar indicates 0.5 μm. **(B)** Effect of rapamycin on mTORC1 activity and autophagy markers in neonatal livers fasted for 10 h. **(C)** Immunofluorescence (IF) of endogenous LC3B in RagA$^{+/+}$ and RagA$^{GTP/GTP}$ MEFs starved of amino acids, as done in Fig. 3e for recombinant LC3B. Bar indicates 10 μm. **(D)** (Top) IF of recombinant TFEB and Lamp2 (as lysosomal marker) in MEFs deprived of amino acids. Bar indicates 10 μm. (Bottom) TFEB transcriptional program is partially impaired in RagA$^{GTP/GTP}$ MEFs upon amino acid withdrawal (n=3; data are mean ± SEM; $p<0.05$). **(E)** Triggering of autophagy by fetal bovine serum (FBS) withdrawal in MEFs. Cells were deprived of FBS for the indicated time points, and whole-cell protein extracts were obtained and mTORC1 activity (S6K, 4E-BP1 and ULK-1 phosphorylation) and LC3B determined by immunoblotting.

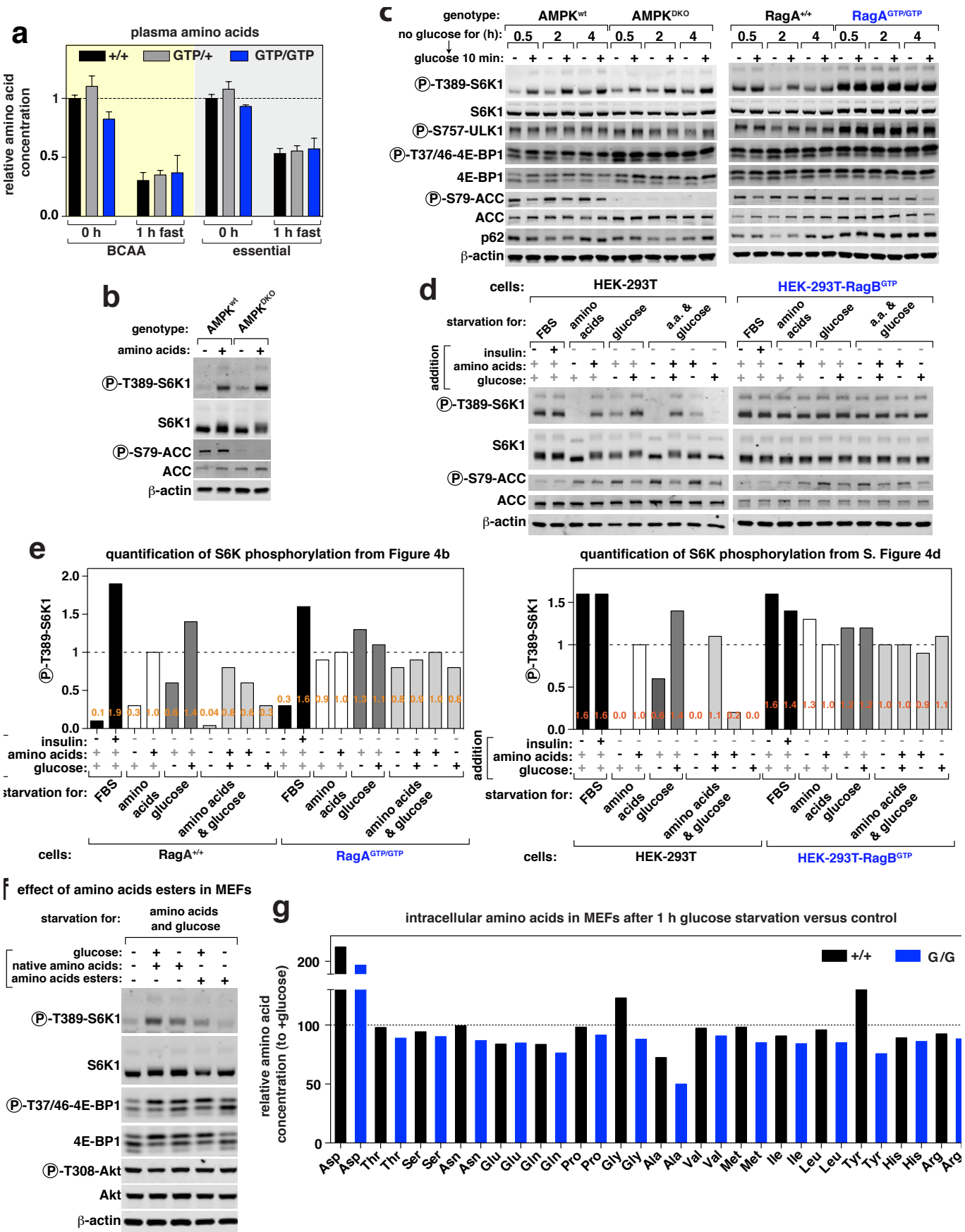
a
plasma amino acids
+/+
GTP/+
GTP/GTP
relative amino acid concentration
0 h
1 h fast
0 h
1 h fast
BCAA
essential
b
genotype:
AMPKwt
AMPKDKO
amino acids:
Ⓟ-T389-S6K1
S6K1
Ⓟ-S79-ACC
ACC
β-actin
c
genotype:
AMPKwt
AMPKDKO
RagA+/+
RagAGTP/GTP
no glucose for (h):
glucose 10 min:
Ⓟ-T389-S6K1
S6K1
Ⓟ-S757-ULK1
Ⓟ-T37/46-4E-BP1
4E-BP1
Ⓟ-S79-ACC
ACC
p62
β-actin
d
cells:
HEK-293T
HEK-293T-RagBGTP
starvation for:
FBS
amino acids
glucose
a.a. & glucose
addition
insulin:
amino acids:
glucose:
Ⓟ-T389-S6K1
S6K1
Ⓟ-S79-ACC
ACC
β-actin
e
quantification of S6K phosphorylation from Figure 4b
Ⓟ-T389-S6K1
insulin:
amino acids:
glucose:
starvation for:
FBS
amino acids
glucose
amino acids & glucose
cells:
RagA+/+
RagAGTP/GTP
quantification of S6K phosphorylation from S. Figure 4d
addition
cells:
HEK-293T
HEK-293T-RagBGTP
f
effect of amino acids esters in MEFs
starvation for:
amino acids and glucose
glucose:
native amino acids:
amino acids esters:
Ⓟ-T389-S6K1
S6K1
Ⓟ-T37/46-4E-BP1
4E-BP1
Ⓟ-T308-Akt
Akt
β-actin
g
intracellular amino acids in MEFs after 1 h glucose starvation versus control
+/+
G/G
relative amino acid concentration (to +glucose)
Asp
Thr
Ser
Asn
Glu
Gln
Pro
Gly
Ala
Val
Met
Ile
Leu
Tyr
His
Arg

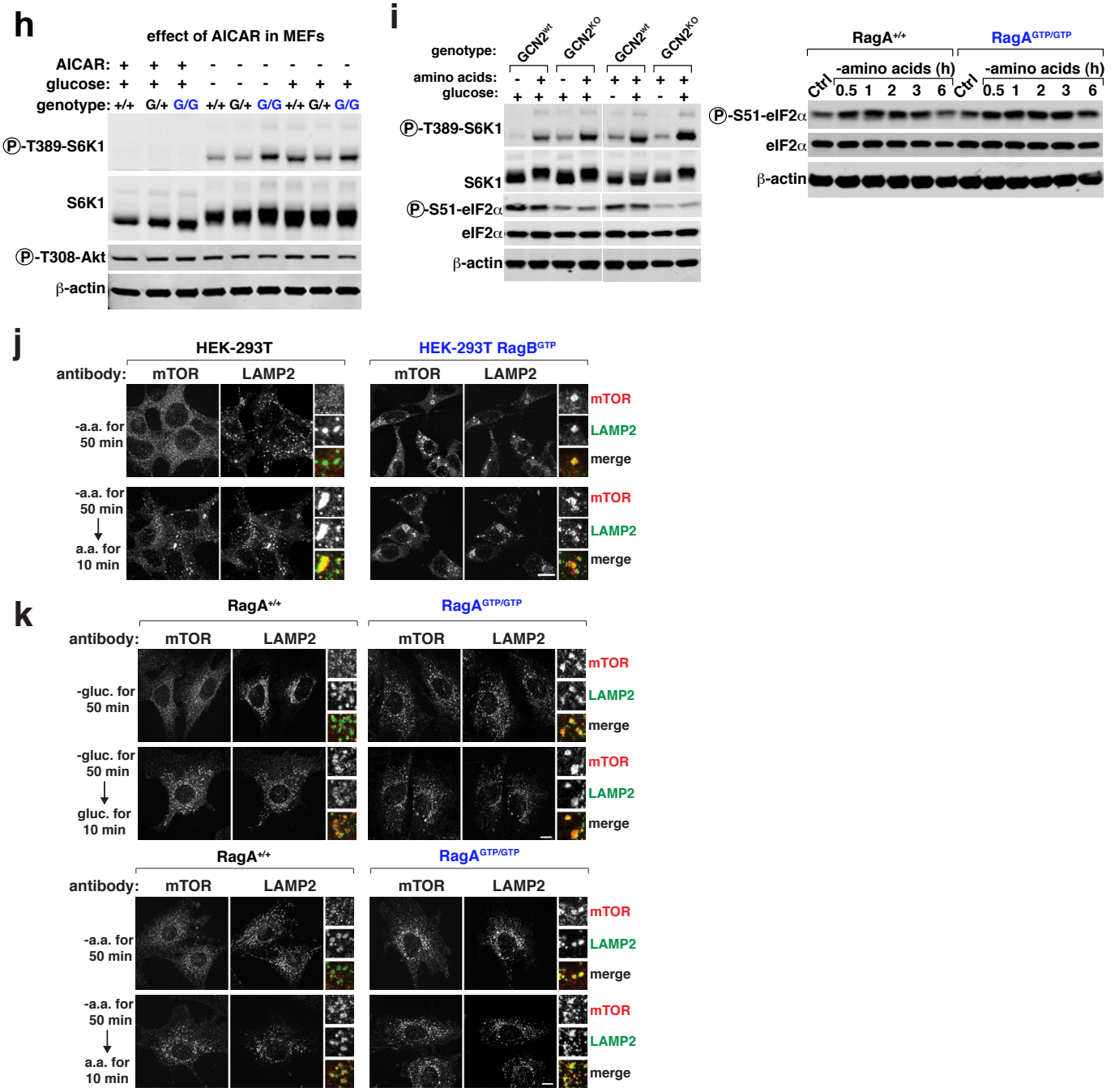

Supplementary Figure 4. (A) Decrease in plasma amino acids in all 1 h fasted neonates, (+/+: n=4 and 3, G/+: n=5 and 6, G/G: n=4 and 4, at 0 h and 1h, respectively, data are mean ± SEM). **(B)** Suppression of mTORC1 activity by amino acid deprivation in AMPK-DKO cells. **(C)** Time course of mTORC1 and AMPK activity in AMPK-wt, AMPK-DKO, RagA$^{+/+}$ and RagA$^{GTP/GTP}$ MEFs deprived of glucose for 0.5, 2 and 4 h. **(D)** Control HEK-293T cells or those expressing RagB^{GTP} were deprived of growth factors, glucose, amino acids, or glucose and amino acids for 1 h and re-stimulated with glucose and/or amino acids for 10 min. Whole cell lysates were analyzed by immunoblotting for the indicated proteins. **(E)** Quantification of the western blots on Figure 4b and Supplementary Fig. 4d. **(F)** Effect of amino acid esters on mTORC1 activity in wt MEFs. **(G)** Quantification of amino acids in RagA$^{+/+}$ and RagA$^{GTP/GTP}$ MEFs deprived of glucose (n=1, relative to un-starved controls). **(H)** Effect of aminoimidazole carboxamide ribonucleotide (AICAR) on mTORC1 activity in RagA$^{+/+}$ and RagA$^{GTP/GTP}$ MEFs. **(I)** (Left) Effect of amino acids or glucose on mTORC1 activity in GCN2-deficient MEFs. (Right) Effect of amino acid deprivation on GCN2 activity in RagA$^{+/+}$ and RagA$^{GTP/GTP}$ MEFs. **(J)** mTOR localization by IF in HEK-293T-RagB^{GTP} and control cells upon amino acid deprivation. **(K)** mTOR localization by IF in RagA$^{+/+}$ and RagA$^{GTP/GTP}$ MEFs deprived of amino acids or glucose. Bar indicates 10 μm.